

# Infrared and THz Soft-Mode Spectroscopy of (Ba,Sr)TiO<sub>3</sub> Ceramics

T. OSTAPCHUK,<sup>1,\*</sup> J. PETZELT,<sup>1</sup> P. KUZEL,<sup>1</sup> S. VELJKO,<sup>1</sup>  
A. TKACH,<sup>2</sup> P. VILARINHO,<sup>2</sup> I. PONOMAREVA,<sup>3</sup>  
L. BELLAICHE,<sup>3</sup> E. SMIRNOVA,<sup>4</sup> V. LEMANOV,<sup>4</sup>  
A. SOTNIKOV,<sup>5,\*\*</sup> AND M. WEIHNACHT<sup>5</sup>

<sup>1</sup>Institute of Physics, Na Slovance 2, 18221 Prague 8, Czech Republic

<sup>2</sup>Department of Ceramics and Glass Engineering, CICECO, University of Aveiro, 3810-193 Aveiro, Portugal

<sup>3</sup>Physics Department, University of Arkansas, Fayetteville, Arkansas 72701, USA

<sup>4</sup>A.I. Ioffe Physical-Technical Institute, Politekhnikeskaya 26, 194021 St. Petersburg, Russian Federation

<sup>5</sup>Leibniz Institute for Solid State and Materials Research Dresden, Helmholtzstrasse 20, 01069 Dresden, Germany

*We performed a study of the temperature dependence of the dielectric response of (Ba,Sr)TiO<sub>3</sub> (BST) ceramics for the whole composition range in a wide frequency range by means of Fourier transform infrared, time-domain THz, microwave and low-frequency dielectric spectroscopy. Room-temperature spectra of the paraelectric dielectric response were compared with the results of first-principle simulations within the effective Hamiltonian approach with a good semi-quantitative agreement. It is shown that in the paraelectric phase away from the transition temperature, the complex THz soft mode, consisting of two overlapping heavily damped oscillators, fully accounts for the low-frequency dielectric properties. However, close to T<sub>C</sub> additional central-mode type dispersion, apparently caused by the pre-transitional polar clusters, is to be expected in the microwave dielectric spectra.*

**Keywords** Soft mode; permittivity; IR reflectivity; Ba<sub>x</sub>Sr<sub>1-x</sub>TiO<sub>3</sub> ceramics

## 1. Introduction

Ba<sub>x</sub>Sr<sub>1-x</sub>TiO<sub>3</sub> (BST-x) is the best studied perovskite ferroelectric solid solution since it is the most perspective tunable high-permittivity materials system for microwave (MW) applications (in the thin film form for varactors) [1]. Due to their difficult growing technique, very few studies were performed on bulk single crystals [2], but quite thorough recent single-crystal Raman scattering study, including the soft-mode behaviour in the

---

Received September 1, 2007.

\*Corresponding author. E-mail: ostapcuk@fzu.cz

\*\*On leave from A.I. Ioffe Physical-Technical Institute, Politekhnikeskaya 26, 194021 St. Petersburg, Russian Federation.

ferroelectric phases, is available for  $x$  up to 0.5 [3]. Most of the results were obtained on bulk ceramics, which are also the subject of our study. The first high-quality ceramics were processed and studied by Smolenski and Rozgatchev [4] and in the modern time the basic experimental information on the phase diagram and dielectric properties (particularly for low  $x$ ) was provided by Lemanov et al. [5] and more recently by Menoret et al. [6]. The rather complicated phase diagram was recently explained in detail by a thermodynamic model based only on the properties of both pure materials by Shirokov et al. [7]. On decreasing  $x$ , the three ferroelectric phases (tetragonal, orthorhombic and rhombohedral) known from the pure BT are merging into a single second-order ferroelectric transition point near 70 K for  $x \cong 0.1$ , which vanishes for  $x < 0.05$  with the appearance of antiferrodistortive phase known from the pure ST at 105 K. The spinodal decomposition and existence of chemical clusters on both ends of the phase diagram (evidenced also experimentally in the low-temperature low- $x$  range [6]) was theoretically predicted by Fuchs et al. [8].

In our recent paper [9] we studied infrared (IR) and THz response of BST- $x$  ceramics for  $x$  up to 0.2 and by comparison of THz and low-frequency permittivity we confirmed the presence of dynamic polar clusters which contribute substantially to the dielectric response in the temperature range of permittivity maxima. Our soft mode data for  $x = 0.2$  were in good agreement with Raman data [3]. For lower  $x$  our softening was not as pronounced as in Raman data, but the evaluation of bulk IR data in the ferroelectric phase is complicated due to the anisotropic grain structure of the ceramics [10].

The soft mode and dielectric behaviour using transverse-field Ising model in combination with Lyddane-Sachs-Teller relations was recently studied by Wu and Shen [11, 12] (particularly at low temperatures where it was in good agreement with  $A_1$ -E averaged Raman soft-mode data [3]). The high-frequency dielectric behaviour including tunability of the permittivity and losses in the MW range, important for applications, was discussed by Vendik et al. [13–15]. Nevertheless, the question of how much amounts the lattice (soft mode) contribution to the MW dielectric response remained open, since no IR soft mode data have been available.

Here we will not refer to many recent papers devoted to BST thin film properties, since these differ appreciably from the bulk behaviour and strongly depend on the substrate and processing [1, 16]. Generally, the ferroelectric soft mode behaviour in ceramics and thin films compared to that in single crystals was discussed in our recent review [10]. Here we present the first IR reflectivity and THz data for the whole composition range of bulk coarse-grain BST ceramics and compare them with low-frequency and MW dielectric data and with the first calculations of the dielectric soft mode response in this system, based on the effective Hamiltonian approach recently used for determining the phase diagram in the whole BST composition and temperature range [17].

## 2. Results and Evaluation

For the present study we have chosen high-density ( $\sim 97\%$ ) BST ( $0.1 \leq x \leq 0.9$ ) ceramic samples prepared by the conventional mixed-oxide route with the calcination at  $1100^\circ\text{C}$  for 2–5 h and final sintering at  $1500^\circ\text{C}$ . The single-phase perovskite structure was checked by the XRD analysis at room temperature. Low-frequency permittivity of all the samples demonstrated a strong dielectric anomaly near the ferroelectric transition with the maximal values of about 15000 comparable to those on single crystals [2] and indicated the presence of three ferroelectric phases for  $x \geq 0.3$  (see Fig. 1). Permittivity measurements, performed in the RF and MW frequency ranges using coaxial technique with impedance analyser (up

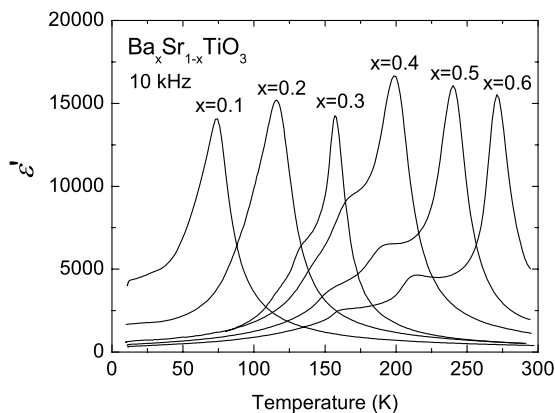


**Figure 1.** Temperature dependences (cooling data) of the low-frequency permittivity for the studied BST- $x$  ceramics up to  $x = 0.6$ .

to 1.8 GHz) [18] and composite resonator technique at 8.8 GHz [19] for  $x \leq 0.6$  do not show any appreciable dispersion in the paraelectric phase as plotted in Fig. 2 for  $x = 0.3$ . Time-domain THz transmission spectroscopy (TDTTS) [20], performed on the polished  $30 \mu\text{m}$  thick plates of  $x \leq 0.4$ , does not reveal permittivity dispersion up to  $\sim 300$  GHz either, but the samples turned out to be opaque in the vicinity of the ferroelectric transformation, where the losses significantly increased, so that only the less-sensitive reflectance measurements could be performed for obtaining the dielectric response. For this purpose we measured the unpolarized reflectivity spectra using Fourier transform IR (FTIR) interferometer Bruker 113v at near-normal specular reflectance. We fitted the obtained spectra (for the example of  $x = 0.3$  see in Fig. 3) with factorised damped harmonic oscillator model to calculate the complex dielectric response [21] (Fig 4). This enabled us to obtain the polar lattice modes contribution to the permittivity in the vicinity of  $T_C$  (for  $x = 0.3$   $T_C \cong 160$  K) but an additional loss mechanism was necessary to be taken into account in the THz region to explain the strong losses which disabled the TDTTS measurements.

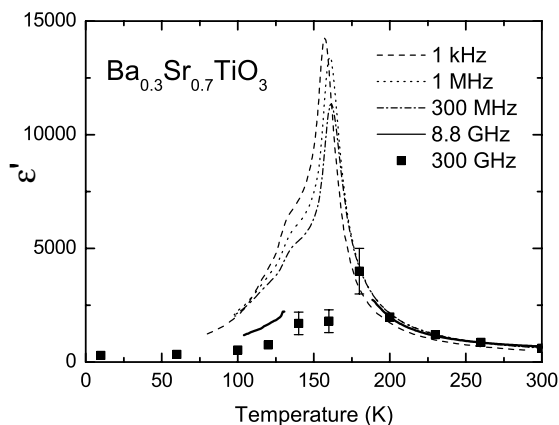


**Figure 2.** Temperature dependence of the permittivity data for  $x = 0.3$  at different frequencies up to the THz range.

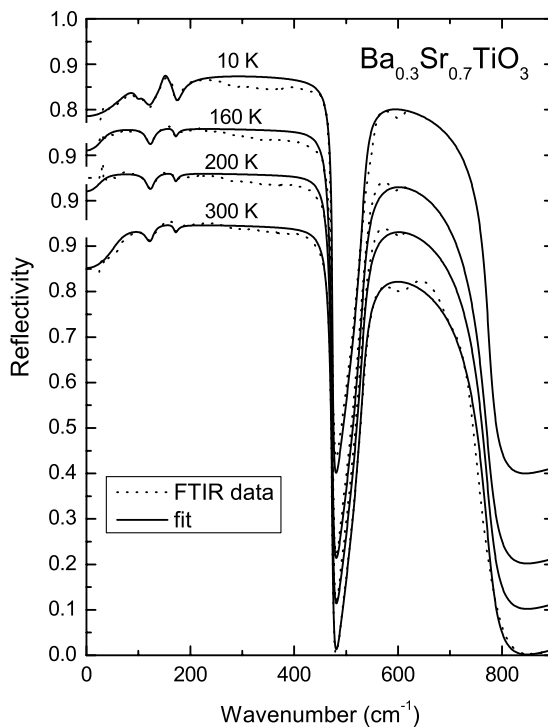


**Figure 3.** Temperature dependence of the IR reflectivity spectra and their fit for  $x = 0.3$ .

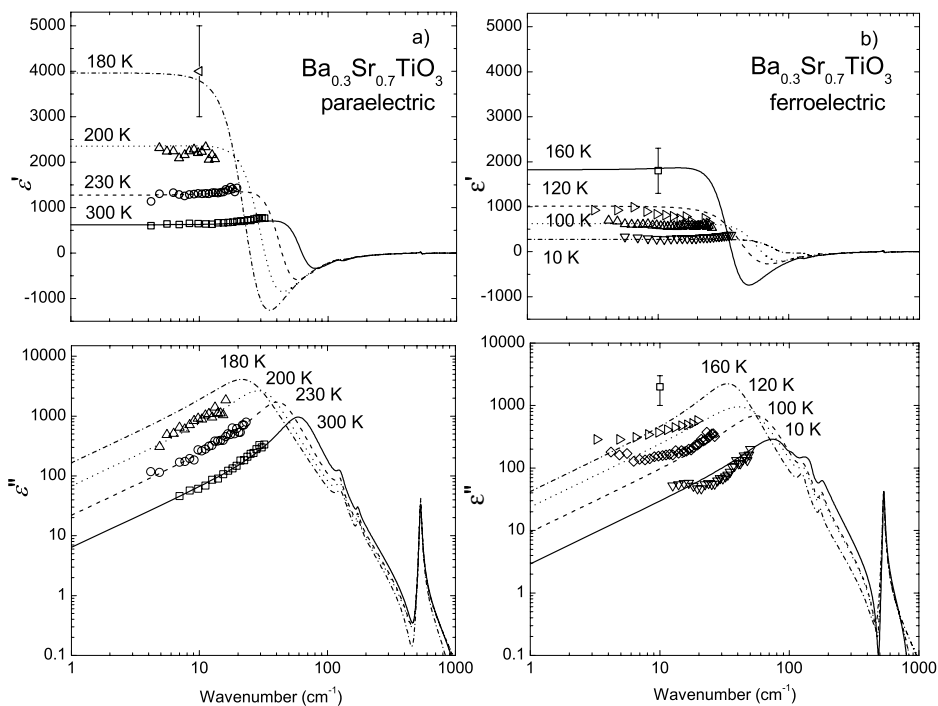


**Figure 4.** Dielectric functions calculated from the fit in Fig. 3.

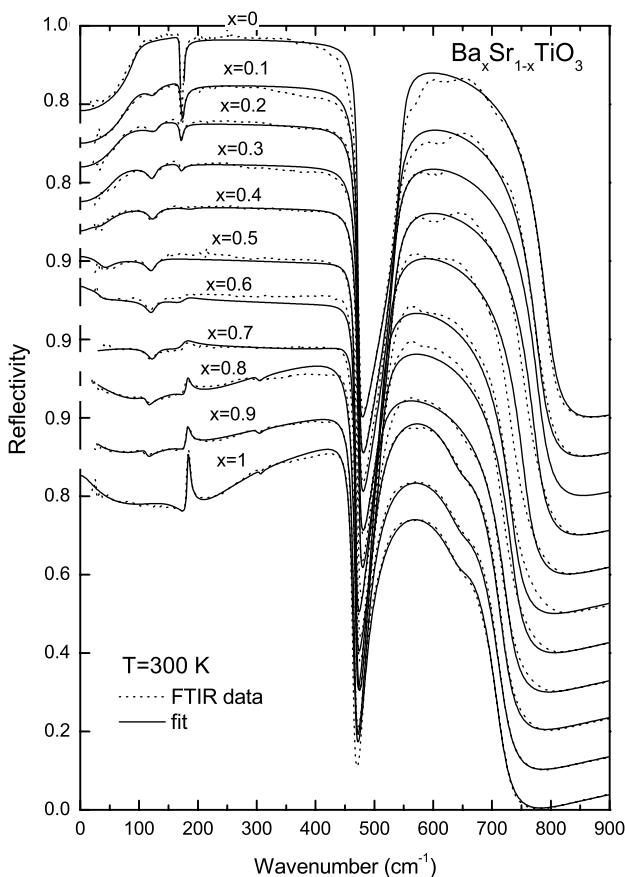


**Figure 5.** Room-temperature FTIR reflectivity spectra of the whole BST system and their fits. The data for both pure compositions are from our previous studies [23, 24].

At room temperature we complemented our FTIR reflectivity data by time-domain THz reflectance spectroscopy (TDTRS) measurements for  $x = 0.5$  and  $0.6$  [22]. FTIR reflectivity spectra and fitting curves obtained with the help of TDTRS and TDTRS data are shown in Fig. 5. The data for both pure compositions are from our previous studies [23] and [24] for ST and BT coarse-grain ceramics, respectively. The corresponding complex permittivity functions calculated from the fits and compared with those calculated using effective Hamiltonian approach and corresponding experimental data are given in Figs. 6–8. In Fig. 9 we summarise our experimental room-temperature paraelectric dielectric soft-mode response on increasing Ba concentration. The data in the ferroelectric phase and their evaluation using the effective dielectric response for anisotropic grains are in progress.

To calculate the complex dielectric response, we have used the approach suggested in Ref. [25], in which the dielectric function is computed from the thermal average of the total dipole moment of the used supercell. We have used supercells of  $14 \times 14 \times 14$  dimensions and the effective Hamiltonian scheme of Ref. [17] to obtain the total dipole moment. Such effective Hamiltonian provides correct transition temperatures for a wide range of Sr concentrations, and was used in molecular dynamics simulation to obtain the total dipole moment of the supercell as a function of time. These data were used to compute

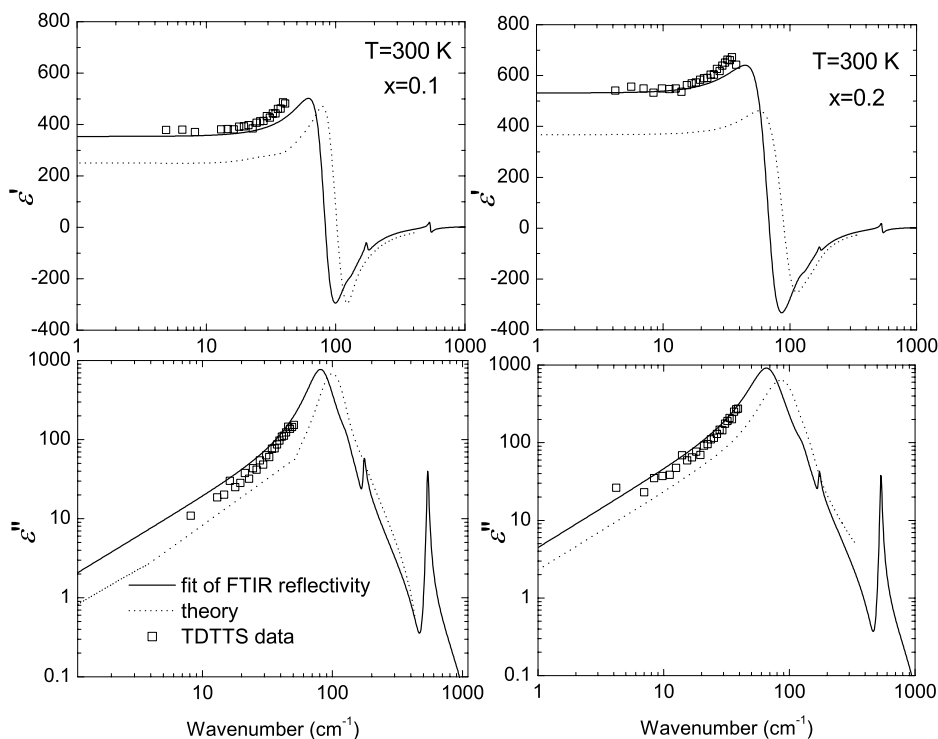


**Figure 6.** Room-temperature complex dielectric function of BST-0.1 and 0.2 ceramics evaluated from our fits compared with theoretical computations.

the dipole-dipole autocorrelation function which was then Fourier transformed to obtain the complex dielectric function. To achieve the desired temperature, we first ran simulations at constant temperature by applying a thermostat and then turned this thermostat off. The time-dependent properties were then collected. More details on the numerical scheme can be found in Ref. [26]. Simulations of disordered BST with different concentration of Sr were carried out by randomly placing the Ba and Sr atoms inside the supercell, according to the desired concentration.

Our computational results at  $T = 300$  K for the paraelectric compositions at higher  $x$  (i.e.,  $0.2 < x < 0.7$ ) show that the imaginary part of the dielectric response has two overlapping peaks. That causes the imaginary part of the response to considerably broaden in the region of comparable Ba and Sr concentration. As the concentration of Sr increases, the lower-frequency peak disappears. Increasing the Sr concentration results in continuous peak(s) shift to higher frequencies, in good agreement with experiments (see Fig. 9).

### 3. Discussion

Comparison of our extrapolated low-frequency permittivity data in Fig. 9 with those directly measured at room temperature (Fig. 1) shows a good agreement for  $x \leq 0.5$ . The permittivity increases with increasing  $x$  since  $T_C$  approaches the room temperature. As expected, the corresponding peak in the dielectric-loss spectra increases and its frequency decreases (mode softens) with increasing  $x$ . However, close to  $T_C$  and in the ferroelectric phase (for

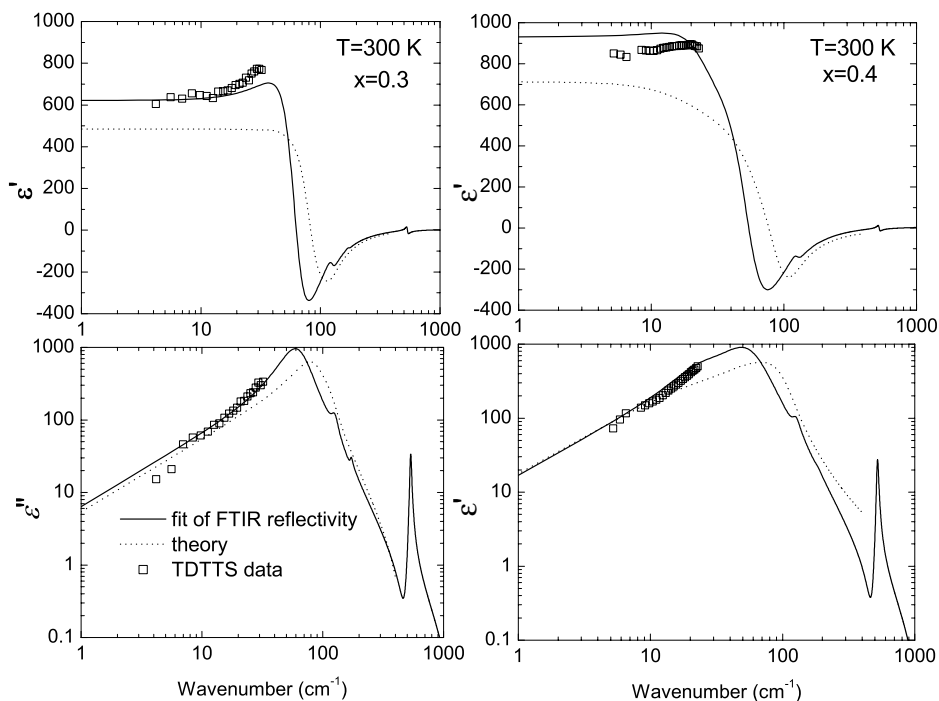


**Figure 7.** Room-temperature complex dielectric function of BST-0.3 and 0.4 ceramics evaluated from our fits compared with theoretical computations.

$x = 0.6$  at and below room temperature and for  $x = 0.3$  below 180 K - see Fig. 2) the measured low-frequency data exceed those extrapolated from the IR-THz fit. Moreover, in the ferroelectric phase a dielectric dispersion is directly seen above the kHz range. This is also in good agreement with our previous data for  $x \leq 0.2$  [9], obtained from different ceramics. The dielectric dispersion in the ferroelectric phase has to be expected due to smeared piezoelectric resonances on grain boundaries and ferroelectric domain-wall contributions. However, the dispersion close but above  $T_C$  (within  $\sim 20$  K) is analogous to dynamic central-mode phenomena appearing often near displacive ferroelectric phase transitions [27, 28]. Since it is not observed in pure ST [23] and BT [24] single crystals as well as in ceramics, it is specific only for BST solid solutions and confirms the existence of dynamic polarization clusters suggested from structural studies [6] as well as from incomplete Raman mode softening [3]. Their characteristic dispersion frequency above  $T_C$  is obviously typically in the 10 GHz range, where any reliable data are still missing since the MW measurements on such high-permittivity and high-loss materials become extremely difficult.

Let us now discuss the spectral line shape of the soft mode at room temperature. For good fits below  $100 \text{ cm}^{-1}$  range we needed 2 heavily damped overlapping oscillators for  $x > 0.2$ , in good agreement with the theoretical simulations. Similar feature, obviously connected with a strong lattice anharmonicity, was recently observed and calculated also in pure BT [26]. Here we only remind that classical two-mode behaviour [29] for the soft mode in BST cannot be expected, because there is obviously no energy gap between the soft phonon spectrum of ST and BT, existence of which appears to be a necessary condition for

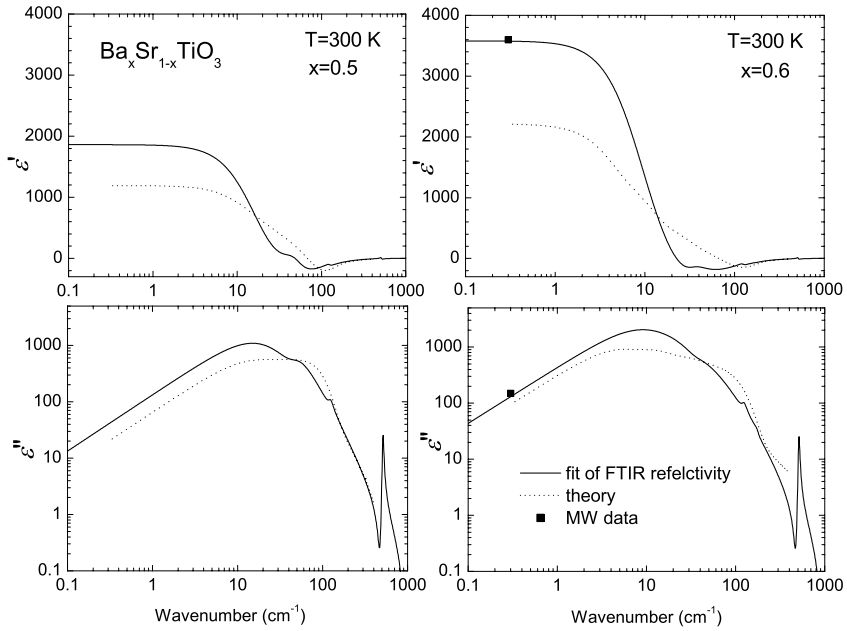


**Figure 8.** Room-temperature complex dielectric function of BST-0.5 and 0.6 ceramics evaluated from our fits compared with theoretical computations.

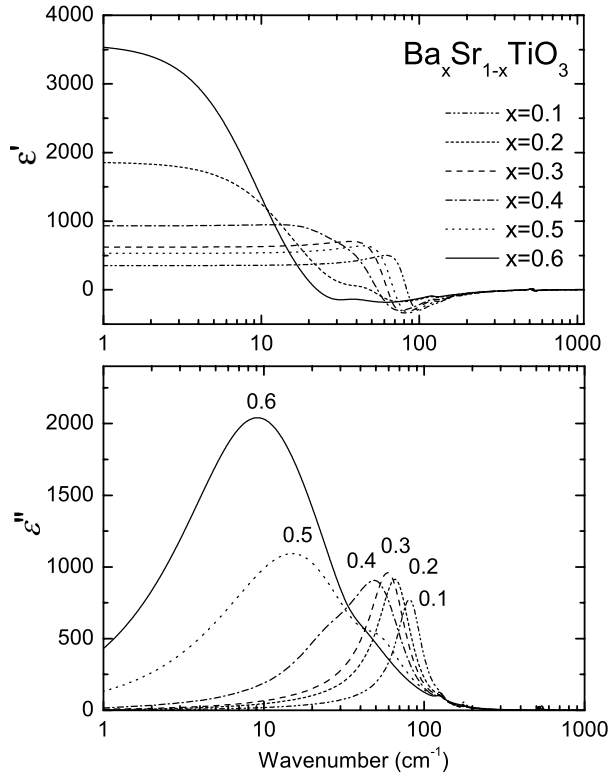


**Figure 9.** Summary of our experimental room-temperature dielectric responses of the BST- $x$  ceramics ( $0.1 \leq x \leq 0.6$ ).

the two-mode behaviour, at least in two-atomic mixed crystals [29, 30]. More quantitative discussion of these features lies outside the scope of this paper. We also note that in all BST samples an additional mode was observed near  $120\text{--}130\text{ cm}^{-1}$  (not present in pure ST and BT), which is revealed in the reflectivity spectra as a distinct minimum (see Fig. 5). This mode was seen also in our previous samples for  $x \geq 0.05$  [9] (denoted as DA), and in Raman spectra [3], where it was assigned to disorder activated non zone-centre phonon. All higher-frequency peaks in our dielectric loss function of BST show non-anomalous one-phonon behaviour. More quantitative conclusions together with temperature dependent behaviour of all modes are in progress.

Concluding, from the analysis of FTIR and THz data we observed imperfect phonon mode softening in all our BST samples, which fully accounts for the paraelectric dielectric behaviour except for a narrow region of  $\sim 20\text{ K}$  above  $T_C$ , where a dynamic central mode in the 10 GHz range is required to contribute to the low-frequency dielectric anomaly. With increasing Ba concentration  $x$  the damping of the soft mode increases and spectral line-shape consists of two peaks in agreement with theoretical calculations based on the model Hamiltonian with one degree of freedom.

## Acknowledgments

The work was supported by the Grant Agency of the Czech Rep. (project No. 202/06/P219) and Academy of Sciences of the Czech Rep. (project AVOZ10100520). One of the authors (T.O.) acknowledges financial support of L'Oreal Fellowship Program "For Women in Science". I.P. and L.B. also acknowledge NSF grants DMR-0701558, DMR-0404335 and DMR-0080054 (C-SPIN), ONR grants N00014-04-1-0413 and N00014-08-1-0915, and DOE grant DE-FG02-05ER46188. E.S. and V.L. acknowledge grants N.Sh.-5169.2006.2, N.Sh.-2628.2008.2 and OFN grant.

## References

1. N. Setter et al., *J. Appl. Phys.* **100**, 051606 (2006).
2. K. Bethe, *Phillips Res. Repts. Suppl.* No2. (1970); K. Bethe, and F. Welz, *Mat. Res. Bull.* **6**, 209 (1971).
3. D. A. Tenne, A. Soukiassian, X. X. Xi, H. Choosuwan, R. Guo, and A. S. Bhalla, *Phys. Rev. B* **70**, 174302 (2004).
4. G. A. Smolenski, and K. I. Rozgatchev, *Zh. Tekh. Fiz.* **24**, 1751 (1954).
5. V. V. Lemanov, E. P. Smirnova, P. P. Syrnikov, and E. A. Tarakanov, *Phys. Rev. B* **54**, 3151 (1996).
6. C. Menoret, J. M. Kiat, B. Dkhil, M. Dunlop, H. Dammak, and O. Hernandez, *Phys. Rev. B* **65**, 224104 (2002).
7. V. B. Shirokov, V. I. Torgashev, A. A. Bakirov, and V. V. Lemanov, *Phys. Rev. B* **73**, 104116 (2006).
8. D. Fuks, S. Dorfman, S. Piskunov, and E. A. Kotomin, *Phys. Rev. B* **71**, 014111 (2005).
9. T. Ostapchuk, M. Savinov, J. Petzelt, A. Pashkin, M. Dressel, E. Smirnova, V. Lemanov, A. Sotnikov, and M. Weihnacht, *Ferroelectrics* **353**, 70 (2007).
10. J. Petzelt, S. Kamba, and J. Hlinka, Ferroelectric soft modes in ceramics and films, in New Developments in Advanced Functional Ceramics, (Ed. L. Mitoseriu) *Transworld Res. Network* **37/661** (2), Fort P. O., Trivandrum, Kerala India 2007, pp. 387-421.
11. H. Wu, and W. Z. Shen, *Appl. Phys. Lett.* **87**, 252906 (2005).
12. H. Wu, and W. Z. Shen, *Phys. Rev. B* **73**, 094115 (2006).
13. O. G. Vendik, E. K. Hollmann, A. B. Kozyrev, and A. M. Prudan, *J. Supercon.* **12**, 325 (1999).
14. O. G. Vendik, and S. P. Zubko, *J. Appl. Phys.* **88**, 5343 (2000).

15. O. G. Vendik, S. P. Zubko, and M. A. Nikolski, *J. Appl. Phys.* **92**, 7448 (2002).
16. R. S. Katiyar, M. Jain, and Yu. I. Yuzyuk, *Ferroelectrics* **303**, 101 (2004).
17. L. Walizer, S. Lisenkov, L. Bellaiche, *Phys. Rev. B* **73**, 144105 (2006).
18. V. Porokhonsky, A. Pashkin, V. Bovtun, J. Petzelt, M. Savinov, P. Samoukhina, T. Ostapchuk, J. Pokorný, M. Avdeev, A. Kholkin, and P. Vilarinho, *Phys. Rev. B* **69**, 144104 (2004).
19. J. Krupka, T. Zychowicz, V. Bovtun, and S. Veljko, *IEEE Trans. Ultrasonics, Ferroelectrics and Freq. Control* **53**, 885 (2006).
20. P. Kuzel, and J. Petzelt, *Ferroelectrics* **239**, 79 (2000).
21. J. Hlinka, J. Petzelt, S. Kamba, D. Noujni, and T. Ostapchuk, *Phase Transit.* **79**, 41 (2006).
22. A. Pashkin, M. Kempa, H. Nemeč, F. Kadlec, and P. Kuzel, *Rev. Sci. Instr.* **74**, 4711 (2003).
23. J. Petzelt, T. Ostapchuk, I. Gregora, I. Rychetský, S. Hoffmann-Eifert, A. V. Pronin, Y. Yuzyuk, B. P. Gorshunov, S. Kamba, V. Bovtun, J. Pokorný, M. Savinov, V. Porokhonsyy, D. Rafaja, P. Vaněk, A. Almeida, M. R. Chaves, A. A. Volkov, M. Dressel, and R. Waser, *Phys. Rev. B* **64**, 184111 (2001).
24. T. Ostapchuk, J. Petzelt, M. Savinov, V. Buscaglia, and L. Mitoseriu, *Phase Transit.* **79**, 361–374 (2006).
25. J.M. Caillol, D. Levesque and J.J. Weis, *J. Chem. Phys.* **85**, 1986 (1986).
26. I. Ponomareva, L. Bellaiche, T. Ostapchuk, J. Hlinka and J. Petzelt, *Phys. Rev. B.* **77**, 012102 (2008).
27. J. Petzelt, G. V. Kozlov, and A. A. Volkov, *Ferroelectrics* **73**, 101 (1987).
28. E. Buixaderas, S. Kamba, and J. Petzelt, *Ferroelectrics* **308**, 131 (2004).
29. I. F. Chang, and S. S. Mitra, *Adv. Phys.* **20**, 359 (1971).
30. J. Petzelt, *Czech. J. Phys. B* **23**, 485 (1973).